Trends in advanced sciences and technology

Trends in Advanced Sciences and Technology

Manuscript 1013

Exergetic Indicators for Evaluation of High Bypass Turbofan Engine at Take-off Condition

Fahad G. AlHarbi

Mohamed H. Mohamed

Bandar M. Fadhl

ORIGINAL STUDY

Exergetic Indicators for the Evaluation of High Bypass Turbofan Engine at Take-off Condition

Fahad G. AlHarbi*, Mohamed H. Mohamed, Bandar M. Fadhl

Department of Mechanical Engineering, College of Engineering and Islamic Architecture, Umm Al-Qura University, Makkah, Saudi Arabia

Abstract

Background: **Aircraft engines consume significant amounts of energy while energy source depletion, climate change, and greenhouse emission effects are rising problems worldwide. Exergy analysis has been a proven useful tool for examining and assessing the performance of different energy systems.**

Method: **In this paper, several exergetic performance indicators are performed to evaluate CFM56-5B3 high bypass turbofan engine components, namely the fan, low-pressure compressor, high-pressure compressor, combustion chamber, high-pressure turbine, low-pressure turbine, and exhaust nozzle at take-off.**

Results and conclusions: **The results indicate that the combustion chamber is the most irreversible component within the engine, with an exergy destruction value of 15.456 MW and an exergy efficiency value of 85.29%. It also has the most exergetic improvement potential among the engine components, with a value of 2.274 MW. In addition, the potential improvement rate is not significant in the exhaust nozzle as it has relatively low exergy destruction of 3.8 kW and excellent exergy efficiency of 98.71%.**

Keywords: Energy, Exergetic indicators, Exergy, Turbofan

1. Introduction

Air transport is vital for global tourism and trade. However, its impact on energy resources and the environment has been a serious issue facing the world. Therefore, it becomes a must to enhance the efficiency and sustainability of energy systems for the well-being of humanity. Considering the importance and growing demand of air transportation for quickness, comfort, and safety aspects to human beings, energy consumption, and climate issues play a critical role in the decision-making and sustainable development of this sector. Consequently, scientists and engineers have been developing more efficient turbofan engines, which can contribute to maintaining energy utilization, reducing environmental pollution, and enhancing the economy.

Exergy analysis stands as a pivotal tool for evaluating the energy efficiency, economic performance, and sustainability of aircraft. It utilizes both the first law and second law of thermodynamics for analyzing, designing, and improving energy systems and applications. It is a useful tool that pinpoints the locations, types, and magnitudes of energy losses in a process, that can lead to more efficient energy use and improved operation. Aircraft engines take a large portion of this analysis since they are the main energy source for the aircraft (Dincer and Rosen, 2012). Researchers have been conducting exergy analyses on aircraft engines to help overcome the current energy, economic, and environmental challenges.

Etele and Rosen (2001) conducted an exergy analysis for a turbojet engine to explore the impact of different reference environments over flight altitudes

Received 21 February 2024; revised 20 May 2024; accepted 3 June 2024.
Available online 24 August 2024

* Corresponding author at: Department of Mechanical Engineering, College of Engineering and Islamic Architecture, Umm Al-Qura University, PO Box 5555, Makkah, Saudi Arabia.
E-mail address: s44280340@st.uqu.edu.sa (F.G. AlHarbi).

https://doi.org/10.62537/2974-444X.1013

ranging from sea level to 15,000 m. Turgut et al. (2007) performed a similar analysis on a low bypass turbofan engine with an afterburner at two altitude levels, which are sea level and 11,000 m altitude level. Turan (2012) performed a specific exergy-based performance for a high bypass turbofan engine at six different reference altitudes ranging from 4000 to 9000 m. Aydin et al. (2013) defined a set of exergo-sustainability indicators, namely exergy efficiency, waste exergy ratio, recoverable exergy rate, exergy destruction factor, environmental effect factor, and exergetic-sustainability index for a turboprop engine at eight flight phases. Additionally, Aydõn et al. (2014) applied an exergetic methodology for a low bypass turbofan engine at maximum power settings. Turan et al. (2014) calculated exergetic measures, namely fuel depletion ratio, productivity lack ratio, fuel exergy factor, product exergy factor, and improvement potential rates for a low bypass turbofan engine at take-off. Tanbay et al. (2015) performed an exergy-based ecological optimization for a single-spool turbofan engine with an unmixed exhaust. Najjar and AbuEisheh (2016) investigated the variation of specific thrust and the specific fuel consumption with different compressor pressure ratios and turbine inlet temperatures by conducting an exergy analysis for a turbojet engine at 13,000 m altitude and 0.8 Mach number. Yucer (2016) conducted an exergy analysis for a small-scale gas turbine jet engine at four different loads, namely idle, part load one, part load two, and full load. Turan and Aydin (2016) carried out an exergo-sustainability analysis for low bypass turbofan engine using six indicators: exergy efficiency, waste exergy ratio, exergetic-sustainability index, environmental effect factor, recoverable exergy rate, and exergy destruction factor. Balli (2017) presented an exergy analysis for a high bypass turbofan engine at take-off using 19 exergetic-sustainability indicators. Balli and Caliskan (2021) investigated aviation, energy, exergy, environmental, and sustainability assessment for a low bypass turbofan engine and its main components. Dinc et al. (2022) conducted a thermodynamic-based enviroeconomic and environmental evaluation of a turboprop engine at seven flight phases. Aygun (2022) computed exergetic, environmental, and sustainability metrics of a turboshaft engine and its components in 10 different settings. Balli (2023) assessed a turboshaft engine using exergy-based environmental and exergy-based sustainability analyses. Aygun (2023) defined exergetic and environmental metrics to evaluate the effect of power settings on a low bypass turbofan engine.

Through a literature review, it is noticed that there are few works about the exergy analysis using exergetic indicators performance to evaluate a high bypass turbofan engine component at maximum power settings (i.e. take-off). Additionally, there is no such work in the open literature for CFM56-5B3 engines. This engine model is employed to propel the extensively utilized narrow-body aircraft, A320 and A321, which are deployed worldwide. Therefore, the current study aims to contribute to the literature and provide a methodology tailored for applying exergy analysis to the CFM56-5B3 engine and identify the quantity and location of the exergy destruction and efficiency for its major components at maximum power setting, that is take-off.

Nomenclature

c_p	specific heat (kJ/kg.K)
$\dot{E}$	energy rate (kW)
ex	specific exergy (kJ/kg)
$\dot{E}x$	exergy rate (kW)
f	relative fuel consumption (%)
h	specific enthalpy (kJ/kg)
$\dot{I}P$	improvement potential rate (kW)
$\dot{m}$	mass flow rate (kg/s)
p	relative product ratio (%)
P	pressure (kPa)
$\dot{Q}$	heat transfer rate (kW)
R	gas constant (kJ/kg.K)
s	specific entropy (kJ/kg.K)
SI	sustainability index
T	temperature (K)
$\dot{W}$	work input (kW)

Subscripts

0	ambient
a	air
ch	chemical
d	destruction
f	fuel
g	combustion gases
in	inlet
k	kth component
kn	kinetic
out	outlet
p	product
ph	physical
pt	potential

Greek symbols

χ	relative exergy destruction (%)
δ	fuel depletion ratio (%)
ε	exergy efficiency (%)
γ	exergy grade function
ξ	productivity lack ratio (%)

2. System description and modeling

CFM56-5B3 is a two-spool high bypass turbofan engine. It is widely utilized to power A320 and A321

aircraft. Its major components include a single-stage fan, a four-stage low-pressure compressor, a nine-stage high-pressure compressor, a single annular combustor in the combustion chamber, a single-stage high-pressure turbine and four-stage low-pressure turbine. The turbofan engine specifications and assumptions used in this study are listed in Table 1.

A diagram illustrating the nomenclature of stations in the turbofan engine is shown in Fig. 1.

Due to the complexity of the engine and to streamline the analysis, the quantities and properties at the preceding component outlet are assumed to be equal to the later component inlet. Therefore, the following listed stations in Table 2 will be considered in the analysis.

2.1. General modeling assumptions

The general modeling and analysis assumptions for the current study are listed as follows (Aydin et al., 2013; Aydõn et al., 2014; Balli, 2014; Turan et al., 2014; Balli, 2017; Balli and Caliskan, 2021):

(1) The temperature and pressure of the environment are taken at 288.15 K and 101.33 kPa, respectively.
(2) Kinetic and potential energy and exergy changes are neglected.
(3) The chemical exergy is neglected except for the combustor.
(4) Air and combustion gases in the engine are treated as perfect gases.
(5) The fan, compressor, and turbine are considered to be adiabatic.
(6) The combustion reaction is complete and stoichiometric.
(7) Pumps, heat exchangers, and bleeding are not included in the analysis.
(8) The type of fuel used is kerosene (JET A1) with a lower heating value of 43,165 kJ/kg and its chemical formula is $C_{12}H_{23}$.

Table 1. Engine specifications and assumptions (CFM International, 2000; Roux, 2007).

Parameters	Value	Unit
SFC	0.0103	kg/kN.s
Airflow	432.2	kg/s
BPR	5.4	
OPR	33.7	
TIT	1500	K
FPR	1.65	
LPCR	2.05	
HPCR	9.95	
HTER	3.74	
LTER	5.56	
Fan isentropic efficiency	86	%
LPC isentropic efficiency	85	%
HPC isentropic efficiency	85	%
HPT isentropic efficiency	91	%
LPT isentropic efficiency	89	%
CC design efficiency	95	%
EN design efficiency	95	%
Mechanical shaft efficiency	99	%

BPR, bypass ratio; CC, combustion chamber; EN, exhaust nozzle; FPR, fan pressure ratio; HPC, high-pressure compressor; HPCR, high-pressure compressor compression ratio; HPT, high-pressure turbine; HTER, high-pressure turbine expansion ratio; LPC, low-pressure compressor; LPCR, low-pressure compressor compression ratio; LPT, low-pressure turbine; LTER, low-pressure turbine expansion ratio; OPR, overall pressure ratio; SFC, specific fuel consumption; TIT, turbine inlet temperature.

2.2. Specific heat of ideal gases

The specific heat of the air (kJ/kg.K) is calculated as a function of temperature using the following (Kotas, 1995):

$$c_{p,a}(T) = 1.04841 - \frac{3.83719}{10^4}T + \frac{9.45378}{10^7}T^2 - \frac{5.49031}{10^{10}}T^3 + \frac{7.92981}{10^{14}}T^4 \quad (1)$$

On a mole basis, dry air is composed of 78.1% N_2, 20.9% O_2, 0.9% Ar, and the remaining 0.1% contains CO_2, He, Ne, and H_2. In combustion processes analysis, Ar can be considered as N_2 and CO_2, He, Ne, and H_2 can be ignored as they exist relatively in a very small amount. Therefore, dry air can be approximated as 21% of O_2 and 79% of N_2 by mole numbers.

Here, the combustion reaction is assumed to be complete in which all carbon and hydrogen in fuel are burned to CO_2 and H_2O, respectively, and there is no C, H_2, CO, or OH in the combustion products. Additionally, the reaction is also assumed to be stoichiometric, in which the fuel is burned with the minimum amount of air needed, and combustion products contain no free O_2. Therefore, the combustion equation of JET A1 fuel ($C_{12}H_{23}$) in terms of mole fractions is calculated as follows (Cengel and Boles, 2014):

$$C_{12}H_{23} + 17.75(O_2 + 3.76N_2) \longrightarrow 12CO_2 + 11.5H_2O + 66.74N_2 \quad (2)$$

After the combustion reaction, the mass percentages of combustion gases are obtained to be 20.27% CO_2, 7.95% H_2O, and 71.77% N_2. The specific heat capacity of hot gases (kJ/kg.K) is given by Cengel and Boles (2014):

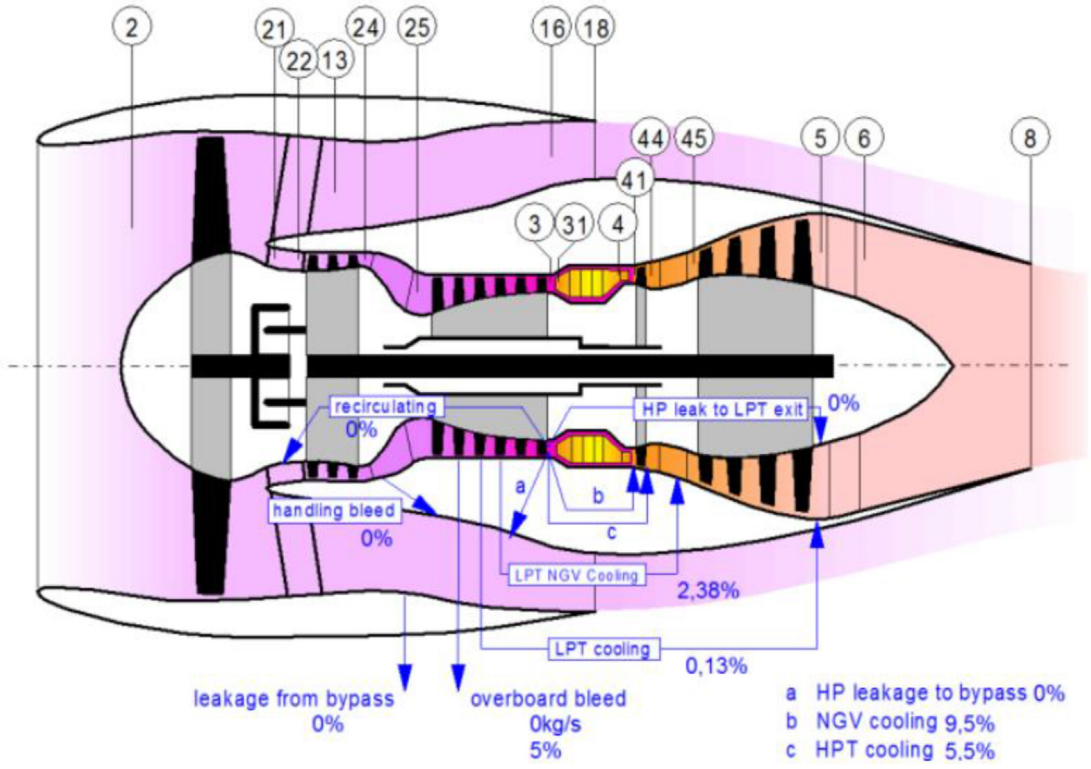

Fig. 1. Station nomenclature of the engine (Kurzke and Halliwell, 2019).

Table 2. Engine stations and their corresponding locations.

Stations	Location
0	Ambient
2	Fan inlet
18	Bypass outlet
21	Core inlet
25	LPC outlet
3	HPC outlet
4	CC outlet
45	HPT outlet
5	LPT outlet
8	Nozzle outlet

CC, combustion chamber; HPC, high-pressure compressor; HPT, high-pressure turbine; LPC, low-pressure compressor; LPT, low-pressure turbine.

$$c_{p,g}(T) = 0.98533 + \frac{0.02438}{10^2}T + \frac{0.00923}{10^5}T^2 - \frac{0.05507}{10^9}T^3 \tag{3}$$

3. Exergy analysis

To model and analyze the system, mass, energy, and exergy balance equations for the control volume system under steady state with neglected kinetic and potential energy changes are presented as follows:

$$\sum \dot{m}_{in} = \sum \dot{m}_{out} \tag{4}$$

$$\dot{Q} - \dot{W} = \sum \dot{m}_{out} h_{out} - \sum \dot{m}_{in} h_{in} \tag{5}$$

$$\sum \left(1 - \frac{T_0}{T}\right)\dot{Q} - \dot{W} = \sum \dot{m}_{out} ex_{out} - \sum \dot{m}_{in} ex_{in} + \dot{E}x_d \tag{6}$$

Here $\dot{m}$ is the mass flow rate (kg/s), $\dot{Q}$ is the heat transfer rate (kW), $\dot{W}$ is the work rate (kW), h is the specific enthalpy (kJ/kg), T is the temperature (K), ex is the specific exergy (kJ/kg), $\dot{E}x_d$ is the exergy destruction rate (kW), and s is the specific entropy (kJ/kg.K). The subscripts *in*, *out*, 0, and *d* refer to inlet, outlet, dead state, and destruction, respectively.

The total exergy in the system can be represented in the form of physical, chemical, potential, and kinetic exergies (Bejan et al., 1995):

$$ex = ex_{ph} + ex_{ch} + ex_{pt} + ex_{kn} \tag{7}$$

The subscripts *ph*, *ch*, *pt*, and *kn* refer to physical, chemical, potential, and kinetic, respectively. In this study, potential and kinetic exergies are neglected. The physical exergy for air and combustion gases at a point is written as:

$$ex_{ph} = h - h_0 - T_0(s - s_0) \tag{8}$$

Assuming air and combustion gases to be perfect gases, the physical exergy can also be calculated using the following:

$$ex_{ph} = c_p(T)\left[T - T_0 - T_0\, ln\frac{T}{T_0}\right] + RT_0\, ln\frac{P}{P_0} \tag{9}$$

Where c_p is the specific heat as a function of temperature (kJ/kg.K), R is the gas constant (kJ/kg.K), and P is the pressure (kPa).

Additionally, the chemical exergy of the fuel (C_aH_b) can be calculated using the following (Moran, 1982; Rakopoulos and Giakoumis, 2006; Balli, 2014):

$$\frac{ex_{ch}}{LHV} = \gamma_f \cong 1.04224 + 0.011925\left(\frac{b}{a}\right) - \frac{0.042}{a} \tag{10}$$

Where γ_f is the liquid fuel exergy grade function.

3.1. Exergetic indicators

It is important to consider exergetic performance indicators in the exergy analysis to evaluate the engine components. In this study, the following indicators are considered in the analysis (Turgut et al., 2009; Balli, 2017, 2014).

Exergy efficiency (ε), which is the ratio of k component outlet exergy to its inlet exergy. It is calculated as follows:

$$\varepsilon_k = \frac{\dot{E}x_{out,k}}{\dot{E}x_{in,k}} \tag{11}$$

Relative exergy destruction (χ) is the ratio of k component exergy destruction to the total exergy destruction of the system. It indicates the percentage of the component exergy destruction as part of the whole system. It is calculated by:

$$\chi_k = \frac{\dot{E}x_{d,k}}{\sum \dot{E}x_d} \tag{12}$$

Fuel depletion ratio (δ) is the ratio of k component exergy destruction to the total fuel exergy supplied to the system. It can be calculated by:

$$\delta_k = \frac{\dot{E}x_{d,k}}{\sum \dot{E}x_f} \tag{13}$$

Relative fuel consumption (f) is the ratio of k component fuel exergy to the total fuel exergy supplied to the system. It is written as:

$$f_k = \frac{\dot{E}x_{f,k}}{\sum \dot{E}x_f} \tag{14}$$

Productivity lack ratio (ξ) is the ratio of k component exergy destruction to the total product exergy of the system. It can be calculated using:

$$\xi_k = \frac{\dot{E}x_{d,k}}{\sum \dot{E}x_p} \tag{15}$$

Relative product ratio (p), which is the ratio of k component product exergy to the total product exergy of the system. It can be found as follows:

$$p_k = \frac{\dot{E}x_{p,k}}{\sum \dot{E}x_p} \tag{16}$$

Improvement potential rate ($\dot{IP}$), which is the rate that defines the maximum available exergetic improvements of k component when exergy destruction is minimized. It is calculated using:

$$\dot{IP}_k = (1 - \varepsilon_k)\dot{E}x_{d,k} \tag{17}$$

The sustainability index (SI) defines the sustainability level of the k component due to emissions based on exergetic efficiency. It is written as follows:

$$SI_k = \frac{1}{1 - \varepsilon_k} \tag{18}$$

4. Results and discussion

A MATLAB code was built to solve the modeling equations. The mass flow rate, temperature, pressure, energy, and exergy of each engine station at take-off conditions are listed in Table 3.

Inlet, outlet, fuel, and product exergy rates, as well as the exergy destruction rate for each component, are presented in Table 4.

The exergy destruction rate for each component is represented in Fig. 2. The maximum exergy destruction rate among the engine components takes place in the combustion chamber with a value of 15,455.99 kW. This owes to the internal irreversibility in the combustion chamber. A similar outcome has been reported in previous works (Aydõn et al., 2014; Balli, 2017; Balli and Caliskan, 2021). The high-pressure and low-pressure turbines are the following components in terms of exergy destruction rates with values of 3549.44 and 3526 kW, respectively. The exhaust nozzle has the lowest exergy destruction rate, 293.7 kW.

Results of exergetic assessment indicators of the engine components are presented in Table 5.

Table 3. Thermodynamic cycle data of the engine at take-off condition.

Stations	Fluid type	$\dot{m}$ (kg/s)	T (K)	P (kPa)	$\dot{E}$ (kW)	$\dot{E}x$ (kW)
0	Air	432.20	288.15	101.33	0	0
2	Air	432.20	288.15	101.33	0	0
18	Air	364.67	339.54	167.19	18,837.04	16,607.80
21	Air	67.53	339.54	167.19	3488.34	3075.52
25	Air	67.53	429.12	342.75	9619.53	8606.28
3	Air	67.53	839.82	3410.35	39,321.41	37,838.55
4	Combustion gases	69.00	1500	3239.83	99,359.82	89,601.73
45	Combustion gases	69.00	1164.56	866.27	69,879.48	55,044.55
5	Combustion gases	69.00	835.17	155.80	41,989.55	22,719.14
8	Combustion gases	69.00	835.17	148.01	41,989.55	22,425.44

Table 4. Exergy rates and exergy destruction for each component.

Components	$\dot{E}x_{in}$ (kW)	$\dot{E}x_{out}$ (kW)	$\dot{E}x_f$ (kW)	$\dot{E}x_p$ (kW)	$\dot{E}x_d$ (kW)
Fan	22,325.38	19,683.32	22,325.38	19,683.32	2642.06
LPC	9197.40	8606.28	6121.88	5530.76	591.12
HPC	39,313.84	37,838.55	30,707.56	29,232.27	1475.29
CC	105,057.72	89,601.73	105,057.72	89,601.73	15,455.99
HPT	89,601.73	86,062.29	34,557.18	31,017.74	3539.44
LPT	55,044.55	51,518.55	32,325.41	28,799.41	3526.00
EN	22719.14	22,425.44	22,719.14	22,425.44	293.70

CC, combustion chamber; EN, exhaust nozzle; HPC, high-pressure compressor; HPT, high-pressure turbine; LPC, low-pressure compressor; LPT, low-pressure turbine.

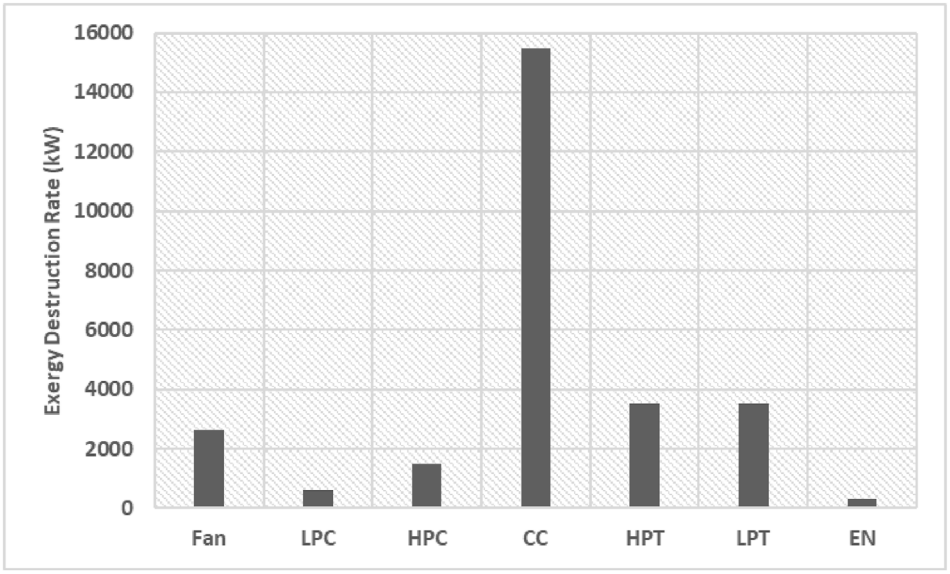

Fig. 2. Exergy destruction rate in each component.

Table 5. Exergetic assessment indicators for each component.

Components	ε (%)	χ (%)	$\dot{I}P$ (kW)	SI	δ (%)	f (%)	ξ (%)	p (%)
Fan	88.17	9.60	312.67	8.45	1.04	8.80	1.17	8.70
LPC	93.57	2.15	57.08	15.56	0.23	2.41	0.26	2.44
HPC	96.25	5.36	70.88	26.65	0.58	12.10	0.65	12.92
CC	85.29	56.16	2273.87	6.80	6.09	41.39	6.83	39.60
HPT	96.05	12.86	362.52	25.32	1.39	13.62	1.56	13.71
LPT	93.59	12.81	384.61	15.61	1.39	12.74	1.56	12.73
EN	98.71	1.07	3.80	77.35	0.12	8.95	0.13	9.91

CC, combustion chamber; EN, exhaust nozzle; HPC, high-pressure compressor; HPT, high-pressure turbine; LPC, low-pressure compressor; LPT, low-pressure turbine.

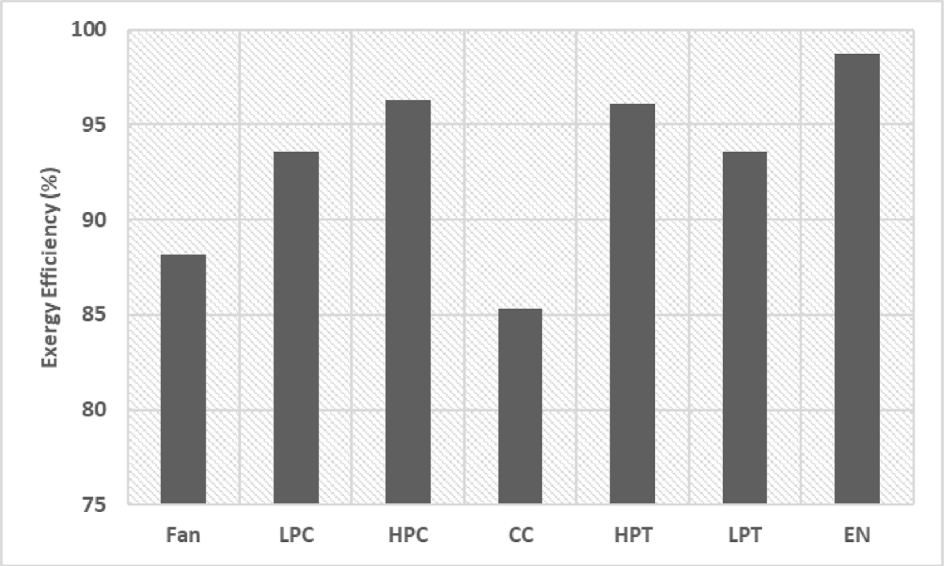

Fig. 3. Exergy efficiency of each component.

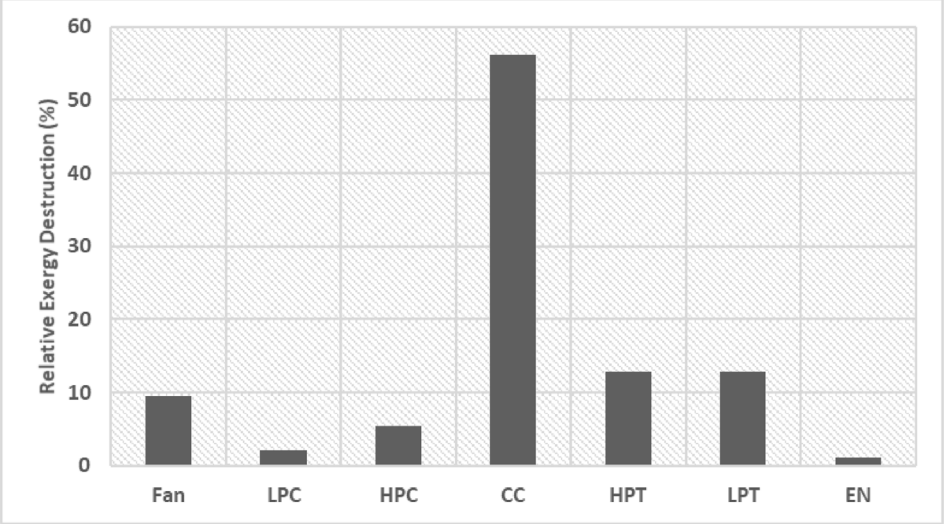

Fig. 4. Relative exergy destruction of each component.

The exergy efficiency of each component is presented in Fig. 3. The results show that the component with the least exergy efficiency is the combustion chamber, with an exergy efficiency value of 85.29%. That is also due to the combustion chamber's irreversibility. On the other hand, the exhaust nozzle is the component with the highest exergy efficiency value of 98.71%. These findings agree with previous studies for other turbofan engines (Balli and Caliskan, 2021). The high and low compressors and turbines' exergy efficiency values are relatively good.

The relative exergy destruction of each component is presented in Fig. 4. It shows clearly that the combustion chamber has the highest relative exergy destruction value of 56.16%. Its relative exergy destruction value alone is more than the total relative exergy destruction value of all the other components, which means that the combustion chamber is responsible for more than half of the exergy destruction within the engine (Balli, 2017; Balli and Caliskan, 2021).

The potential improvement of each component is presented in Fig. 5. The combustion chamber shows very promising exergetic potential improvement with a value of 2273.87 kW. The combustion chamber has been reported with the highest potential improvement value among the engine components

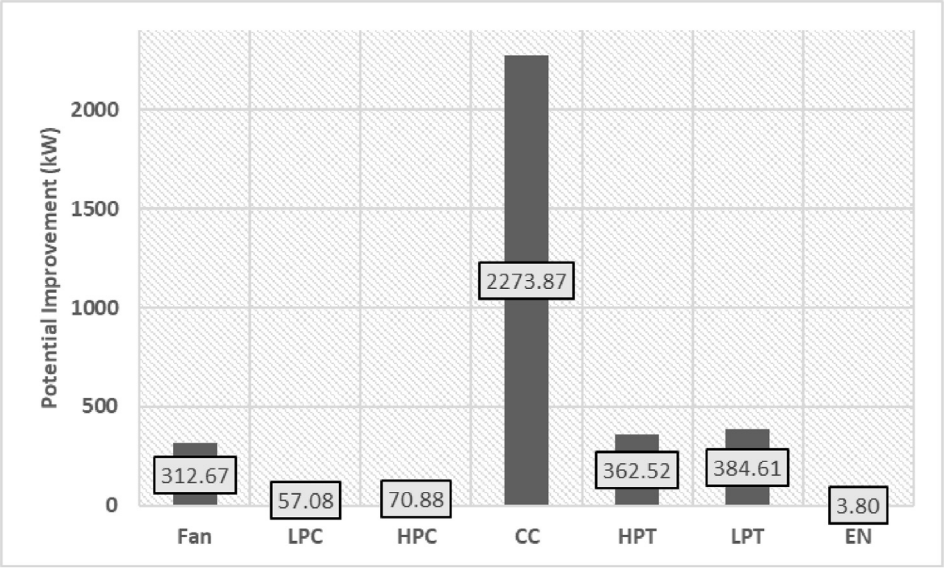

Fig. 5. Potential improvement of each component.

(Turan et al., 2014; Balli, 2017; Balli and Caliskan, 2021; Aygun, 2023). In contrast, the exhaust nozzle has the lowest potential improvement, with a value of 3.80 kW. The results can be owed to the fact that the exhaust nozzle has excellent exergy efficiency with relatively low exergy destruction. The same principle can be applied to the low-pressure compressor.

The sustainability index of each component is presented in Fig. 6. The illustration shows that the exhaust nozzle has the highest sustainability index among the engine components, with a value of 77.35. The combustion chamber has the lowest sustainability index, with a value of 6.8. This is due to the fact that the combustion chamber has the lowest exergy efficiency, hence, it has a low sustainable level and vice versa. The sustainability index of the combustion chamber has also been the lowest value among the engine components (Balli, 2017; Balli and Caliskan, 2021).

The fuel depletion ratio of each component is presented in Fig. 7. The combustion chamber was the component with the highest depletion ratio value of 6.09%. It was relatively very high compared

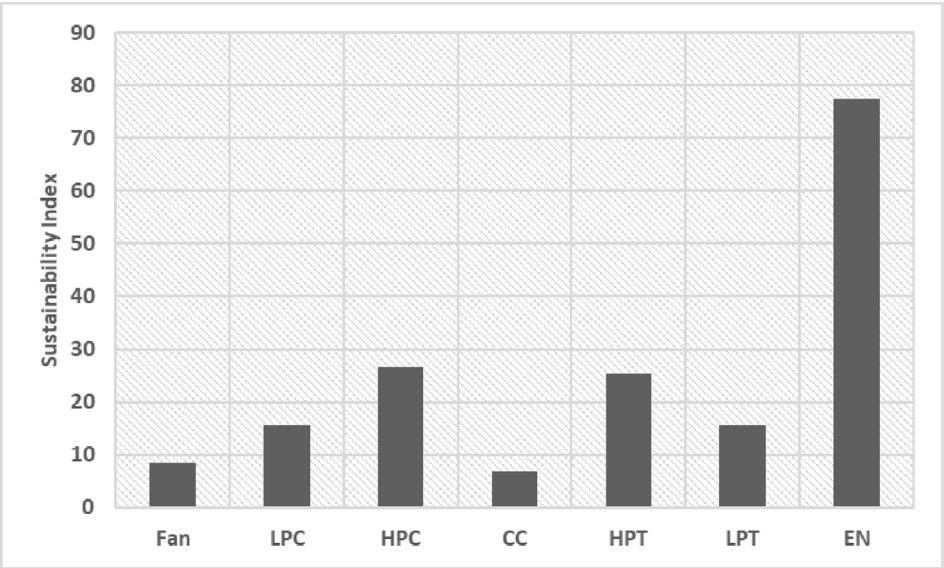

Fig. 6. Sustainability index of each component.

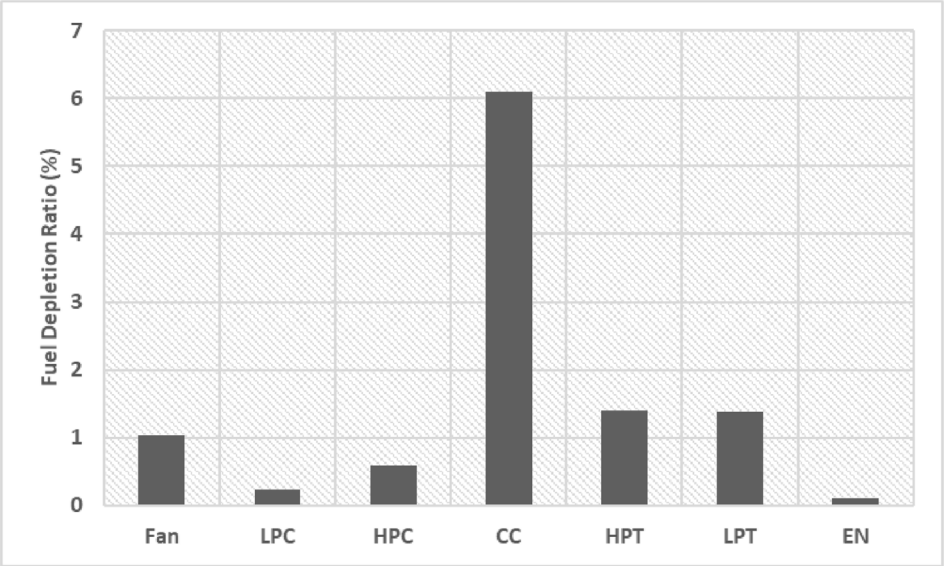

Fig. 7. Fuel depletion ratio of each component.

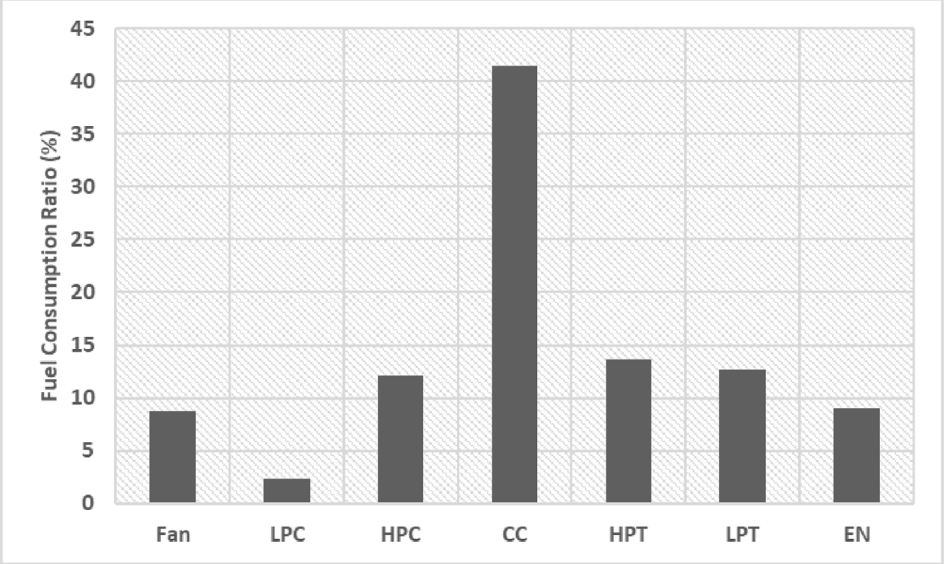

Fig. 8. Fuel consumption ratio of each component.

to the other components (Turan et al., 2014; Balli, 2017). The exhaust nozzle, on the other hand, was the one with the lowest fuel depletion ratio value of 0.12%. About 10% of the fuel exergy is wasted within the engine components, and about 60% of this quantity comes from the combustion chamber.

Similarly, the fuel consumption ratio of each component is shown in Fig. 8. The combustion chamber is the most consumer of fuel exergy (Turan et al., 2014; Balli, 2017; Balli and Caliskan, 2021; Aygun, 2023), with 41.39% of the total fuel exergy within the system. The low-pressure compressor is the least used unit at 2.41%.

The productivity lack ratio of each component is illustrated in Fig. 9. About 12.16% of the product's exergy potential is lost within the system. More than half of this quantity comes from the combustion chamber. The productivity lack ratio of the combustion chamber was relativity high (Turan et al., 2014; Balli, 2017; Balli and Caliskan, 2021).

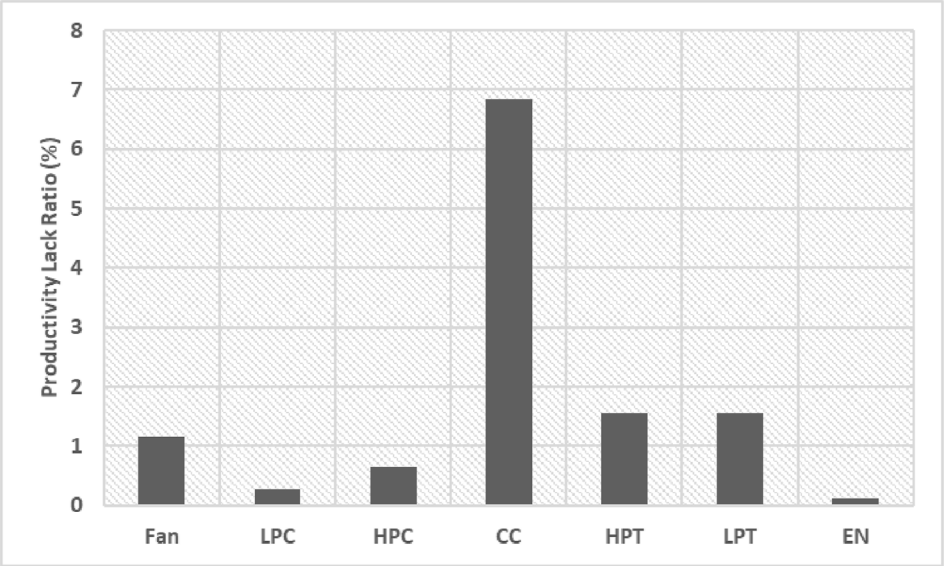

Fig. 9. Productivity lack ratio of each component.

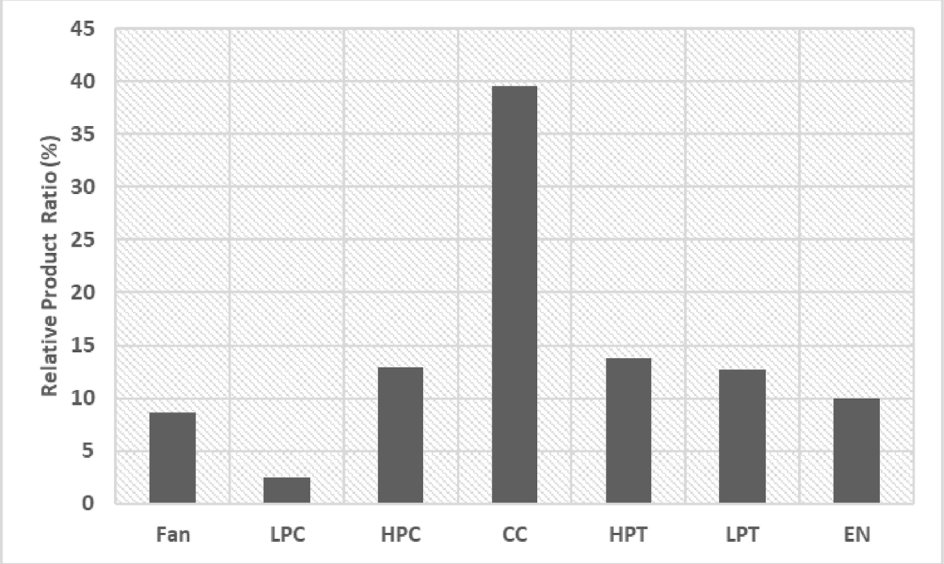

Fig. 10. Relative product ratio of each component.

Similarly, the relative product ratio of each component is shown in Fig. 10. The combustion chamber produces most of the total product exergy within the system, reported as the highest (Turan et al., 2014; Balli, 2017; Balli and Caliskan, 2021; Aygun, 2023) with a value of 39.6%. In contrast, the low-pressure compressor produces 2.44% of the total product exergy.

4.1. Conclusion

This study presents an exergy analysis for the CFM56-5B3 turbofan engine at take-off. The main conclusions of the study are summarized as follows:

(1) The combustion chamber has the highest exergy destruction rate within the system, with a value of 15,455.99 kW, and it is also responsible for more than half of the exergy destruction within the system. This is due to the irreversibility of this component.
(2) The combustion chamber is the least efficient component, with a value of 85.29%. Nevertheless, it shows a very promising potential improvement rate value of 2273.87 kW.

(3) The potential improvement rate is not significant if a component, such as the exhaust nozzle, has excellent exergy efficiency with relatively low exergy destruction.
(4) The combustion chamber has the least sustainable level, with a 6.8 value on the sustainability index within the system components.
(5) The combustion chamber is the most consumer of fuel exergy and also the most producer of product exergy within the system, with values of 41.39 and 36.6%, respectively. About 10% of the fuel exergy is wasted within the system, and about 60% of it takes place in the combustion chamber. Furthermore, about 12.16% of the product exergy potential is lost within the system, and more than half of it is caused by the combustion chamber.

Lastly, an advanced exergy analysis for the current system is useful for future work. It helps to investigate the relationships among the present model components to avoid exergy destruction.

Funding

The authors didn't receive any funding support.

Conflicts of interest

There are no conflicts of interest.

References

Aydin, H., Turan, Ö., Karakoç, T. H., & Midilli, A. (2013). Exergo-sustainability indicators of a turboprop aircraft for the phases of a flight. *Energy, 58*, 550–560.
Aydõn, H., Turan, O., Midilli, A., & Karakoc, T. H. (2014). Exergetic performance of a low bypass turbofan engine at takeoff condition. *Progress in Exergy, Energy, and the Environment*, 293–303.
Aygun, H. (2022). Thermodynamic, environmental and sustainability calculations of a conceptual turboshaft engine under several power settings. *Energy, 245*, Article 123251.
Aygun, H. (2023). Dealing with aspects of performance and environmental impact of aircraft engine with thermodynamic metrics. *Sakarya University Journal of Science, 27*, 370–385.
Balli, O. (2014). Afterburning effect on the energetic and exergetic performance of an experimental turbojet engine (TJE). *International Journal of Exergy, 14*, 212–243.
Balli, O. (2017). Exergy modeling for evaluating sustainability level of a high by-pass turbofan engine used on commercial aircrafts. *Applied Thermal Engineering, 123*, 138–155.
Balli, O. (2023). Exergetic, sustainability and environmental assessments of a turboshaft engine used on helicopter. *Energy, 276*, Article 127593.
Balli, O., & Caliskan, H. (2021). Turbofan engine performances from aviation, thermodynamic and environmental perspectives. *Energy, 232*, Article 121031.
Bejan, A., Tsatsaronis, G., & Moran, M. J. (1995). *Thermal design and optimization*. John Wiley & Sons.
Cengel, Y. A., & Boles, M. A. (2014). *Thermodynamics: an engineering approach*. McGraw-Hill Higher Education.
CFM International. (2000). *CFM56-5B Training Manual for Basic Engine*.
Dinc, A., Caliskan, H., Ekici, S., & Sohret, Y. (2022). Thermodynamic-based environmental and enviroeconomic assessments of a turboprop engine used for freight aircrafts under different flight phases. *Journal of Thermal Analysis and Calorimetry, 147*, 12693–12707.
Dincer, I., & Rosen, M. (2012). *Exergy: energy, environment, and sustainable development*. Elsevier.
Etele, J., & Rosen, M. A. (2001). Sensitivity of exergy efficiencies of aerospace engines to reference environment selection. *Exergy, 1*, 91–99.
Kotas, T. J. (1995). *The exergy method of thermal plant analysis*. Krieger.
Kurzke, J., & Halliwell, I. (2019). *Propulsion and power: An exploration of gas turbine performance modeling*. Springer.
Moran, M. J. (1982). *Availability analysis: A guide to efficient energy use*. Prentice Hall.
Najjar, Y. S., & AbuEisheh, H. (2016). Exergy analysis and greening performance carpets for turbojet engines. *Journal of Engineering and Thermophysics, 25*, 262–274.
Rakopoulos, C., & Giakoumis, E. (2006). Second-law analyses applied to internal combustion engines operation. *Progress in Energy and Combustion Science, 32*, 2–47.
Roux, E. (2007). In Elodie Roux (Ed.), *Turbofan and turbojet engines: Database handbook*. Paris.
Tanbay, T., Durmayaz, A., & Sogut, O. S. (2015). Exergy-based ecological optimisation of a turbofan engine. *International Journal of Exergy, 16*, 358–381.
Turan, O. (2012). Effect of reference altitudes for a turbofan engine with the aid of specific-exergy based method. *International Journal of Exergy, 11*, 252.
Turan, O., & Aydin, H. (2016). Exergy-based sustainability analysis of a low-bypass turbofan engine: a case study for JT8D. *Energy Procedia, 95*, 499–506.
Turan, O., Aydõn, H., Karakoc, T. H., & Midilli, A. (2014). Some exergetic measures of a JT8D turbofan engine. *J Automat Control Eng, 2*, 110–114.
Turgut, E. T., Karakoc, T. H., & Hepbasli, A. (2007). Exergetic analysis of an aircraft turbofan engine. *International Journal of Energy Research, 31*, 1383–1397.
Turgut, E. T., Karakoc, T. H., Hepbasli, A., & Rosen, M. A. (2009). Exergy analysis of a turbofan aircraft engine. *International Journal of Exergy, 6*, 181–199.
Yucer, C. T. (2016). Thermodynamic analysis of the part load performance for a small scale gas turbine jet engine by using Exergy Analysis Method. *Energy, 111*, 251–259.